Published in final edited form as:
Gene Expr Patterns. 2009 June ; 9(5): 255–265. doi:10.1016/j.gep.2009.04.002.

BMP and BMP receptor expression during murine organogenesis

Shahab M. Danesh, **Alethia Villasenor**, **Diana Chong**, **Carrie Soukup**, and **Ondine Cleaver***
Department of Molecular Biology, University of Texas Southwestern Medical Center, 5323 Harry Hines Blvd., Dallas, Texas, USA 75390

Abstract

Cell-cell communication is critical for regulating embryonic organ growth and differentiation. The Bone Morphogenetic Protein (BMP) family of transforming growth factor β (TGFβ) molecules represents one class of such cell-cell signaling molecules that regulate the morphogenesis of several organs. Due to high redundancy between the myriad BMP ligands and receptors in certain tissues, it has been challenging to address the role of BMP signaling using targeting of single *Bmp* genes in mouse models. Here, we present a detailed study of the developmental expression profiles of three BMP ligands (*Bmp2*, *Bmp4*, *Bmp7*) and three BMP receptors (*Bmpr1a*, *Bmpr1b*, and *BmprII*), as well as their molecular antagonist (*noggin*), in the early embryo during the initial steps of murine organogenesis. In particular, we focus on the expression of Bmp family members in the first organs and tissues that take shape during embryogenesis, such as the heart, vascular system, lungs, liver, stomach, nervous system, somites and limbs. Using in situ hybridization, we identify domains where ligand(s) and receptor(s) are either singly or co-expressed in specific tissues. In addition, we identify a previously unnoticed asymmetric expression of *Bmp4* in the gut mesogastrium, which initiates just prior to gut turning and the establishment of organ asymmetry in the gastrointestinal tract. Our studies will aid in the future design and/or interpretation of targeted deletion of individual *Bmp* or *Bmpr* genes, since this study identifies organs and tissues where redundant BMP signaling pathways are likely to occur.

Keywords

Organogenesis; Bmp2; Bmp4; Bmp7; Bmpr1a; Bmpr1b; BmprII; Noggin; heart; lung; gut; stomach; limb bud; neural fold; somite

INTRODUCTION

Morphogenesis of embryonic tissues and initiation of organogenesis begins post-grastulation around embryonic day 8 (E8.0) in the mouse, with the onset of heart and blood vessel development. Over the next 24 hours, the embryonic endoderm transforms from a single cell layer sheet into an open cylinder which rapidly zippers up into the gastrointestinal tract and associated umbilical cord. Coordinately, the embryo undergoes ‘turning’, as it twists on its axis and acquires its characteristic fetal shape. In addition, during this time, most organs appear along the anteroposterior axis, including the budding pituitary, thyroid, salivary glands, lung,

*Address correspondence to: Ondine Cleaver, Department of Molecular Biology, NA8.300, University of Texas Southwestern Medical Center, 5323 Harry Hines Blvd., Dallas Texas 75390-9148, USA. Phone: (214) 648-1647; Fax (214) 648-1196; E-mail: E-mail: ondine.cleaver@utsouthwestern.edu.

liver and pancreas. During the next 48hrs these organs continue to develop and take shape, and in the strikingly short span of approximately two days (E8.0–E10.5), the principal embryonic organs have become specified and emerged from relatively simple germ layers (ectoderm, mesoderm and endoderm), and undergone morphogenesis resulting in complex, multi-cellular organs. This dynamic process is ultimately the result of step-wise cell differentiation that involves a busy crosstalk of cell-cell signaling between growing tissues and the interplay of numerous different intrinsic gene pathways. A number of extrinsic factors have been shown to interact and drive organ and tissue formation during embryonic development, including the Wnt, hedgehog (Hh), fibroblast growth factor (Fgf), Notch, and transforming growth factor β (TGFβ/bone morphogenetic protein (BMP) families of signaling molecules. Our studies focus on the BMP growth factor family and the expression of Bmps during organogenesis.

Bone morphogenetic proteins (BMPs) are part of the TGF-β superfamily (Kingsley, 1994) and comprise a large, evolutionarily conserved family of secreted signaling molecules that are required for numerous developmental processes. BMPs were originally isolated because of their capacity to promote bone and cartilage formation (Urist, 1965). However, they have also been shown to participate in the establishment of the initial vertebrate body plan, somite and neural tube patterning, as well as the development of a large number of structures and organs, such as kidney, lung, liver, limb, amnion, eye, teeth, pituitary, and testes (reviewed in (Hogan, 1996; Zhao, 2003). The importance of the development function of these BMP factors is highlighted by the fact that deletion of many Bmp genes (including *Bmp2* and *Bmp4*) and their receptors (including *Bmpr1a* and *II*) results in early embryonic lethality (prior to E9.5) when most gastrointestinal organs are just beginning to initiate development (reviewed in (Zhao, 2003). Although conditional ablation of *Bmpr1a* has demonstrated its specific requirement in a number of tissues (Eblaghie et al., 2006; Park et al., 2006), the specific roles of BMP ligands and other BMP receptors have yet to be described.

BMPs, like other TGFβs, are first synthesized and folded in the cytoplasm and subsequently cleaved by proteases during secretion. BMPs form large, dimeric proteins, whose proper conformation is required for their receptor binding and biological action (Eimon and Harland, 1999). In mouse, a single BMP type II receptor subunit (BMPRII) has been identified (Beppu et al., 1997), while at least three type I receptors have been found (BMPR1a/Alk3, BMPR1b/Alk6 and ActRIa/Alk2) (ten Dijke et al., 1994). After BMP ligand binding, BMPRII heterodimerizes with a type I receptor, such as BMPR1a or BMPR1b, resulting in type II receptor phosphorylation and activation of the type I receptor. The type I receptor in turn phosphorylates cytoplasmic downstream target proteins, including Smad family proteins (see review (Kretzschmar and Massague, 1998) which act as transcription factors and regulate many downstream pathways. Adding to BMP signaling complexity, BMPs can also interact with type II activin receptors ActRIIa and ActRIIb (Yamashita et al., 1995). Therefore, as BMPs display promiscuity in binding affinities and their receptors function as heterodimers, multiple possible signaling cascades exist and depend on the expression of specific BMP ligands and receptors in given tissues.

Bmp ligand and receptor expression profiles have been described in scattered reports in the literature (Bitgood and McMahon, 1995; Dewulf et al., 1995; Furuta et al., 1997; Jones et al., 1991; Lyons et al., 1995; Solloway and Robertson, 1999), however, a comprehensive comparative gene expression analysis has not been described for the decapentaplegic (*dpp*) subgroup of Bmp genes (*Bmp2*, *Bmp4*) and their receptors (*Bmpr1a*, *Bmpr1b* and *BmprII*) throughout organogenesis. Myriad reports have demonstrated the critical importance of both Bmp ligands and their receptors for embryonic organ and tissue development. In particular, elegant conditional deletion studies have shown the requirement for *Bmp4* (Kulessa and Hogan, 2002), *BmpRII* (Beppu et al., 2005) and *BmpR1a* (Mishina et al., 2002) in a number of tissues including the cardiovascular system (Kaneko et al., 2008; Park et al., 2006; Yu et al., 2005),

lung (Eblaghie et al., 2006), limb (Ovchinnikov et al., 2006), central nervous system and many more. In this report, we analyze expression of *Bmp2*, *Bmp4*, *Bmp7* and their receptors *Bmpr1a*, *Bmpr1b*, and *BmprII*, and the BMP antagonist *noggin*, prior to and during organogenesis, with special focus on tissues where multiple ligands and receptors are co-expressed at distinct timepoints. These studies will help elucidate interpretations of genetic deletion studies that may be complicated by tissue specific BMP signaling redundancy. We employ in situ hybridization to examine and compare expression of transcripts of these genes, in postgastrulation embryos from stages E7.5 to E10.5. We aim to identify sites where single or multiple BMPs may play a role during organogenesis.

RESULTS AND DISCUSSION

Bmp2- E7.25 to E10.5

We initially assayed expression of Bmp genes using whole mount in situ hybridization. (For all descriptions of gene expression in embryonic organs and tissues refer to structure annotations found in top panels of each figure, either in schematic or overlaid on photographed embryo, and associated organ or tissue name in figure legends). Our analysis of Bmp gene expression began at E7.25, a time in development when embryonic tissues start to form following gastrulation. We find that at this stage, *Bmp2* is primarily expressed in the yolk sac (y) and allantois (a), in the precardiac crescent (cc), just anterior to the anterior intestinal portal, or AIP (aip) (Fig. 1A1). Expression appears distinctly absent in the medial, open gut region (g) of the embryo, which includes pre-somitic mesoderm, endoderm, and neural tissues. By E8.25, we observe an increase in *Bmp2* expression in the linear heart tube (h) and allantois, while high levels of expression are observed in the constricting AIP and sinus venosus (sv), regions immediately ventroposterior to the heart (Fig. 1A2). In addition, strong expression initiates in the dorsal most tip of the rostroanterior neural folds (nf) and the midline fusion point of the neural folds spanning the length of the embryo. Expression also appears robustly in the lateral plate mesoderm (lpm).

Slightly later, at E8.75, expression remains strong in the sinus venosus and in the fusing dorsal neural tube (Fig. 1A3, Fig. 2A1 and Fig. 3A1). Strikingly, rather significant expression is also detected in the heart, shortly after the heart takes shape and starts to loop. Expression is particularly strong in the region that joins the left ventricle and the atria, which will later give rise to the atrioventricular canal region, or AVC (avc) (arrow in Fig. 1A3), a region previously shown to express both *Bmp2* and *Tbx2* (Christoffels et al., 2004). Expression is also high in the pericardium, with declining expression in the ‘seam’ of the dorsal brain, which represents the region of the midline fusion of the anterior neural folds.

Later, at E9.0, *Bmp2* remains strongly expressed in the AVC, but has declined from the midline seam of the telencephalon (ms) (Fig. 1A4, Fig. 2A2 and Fig. 3A2). In addition, expression has decreased in the constricting base of the yolk sac (ysc) (or the future umbilical cord), and associated lateral plate mesoderm, as embryonic turning proceeds and the gut tube forms (Fig. 1A4). Expression is low in the head and branchial arches, as well as the dorsal neural tube at this stage of development. Expression remains strong in the liver diverticulum (l) (Fig. 1A4 and Fig. 2A2). *Bmp2* also increases expression in the developing forelimbs (lb) (Fig. 2A3 and Fig. 3A3), the rostral dorsal aortae (ao) of the trunk and the anterior tip of the developing mesenephros (m) (arrowheads in Fig. 1A4).

At E9.5, *Bmp2* has also begun to be expressed in the apical ectodermal ridge, or AER (aer), of the limb bud, a region long noted for its organizing activity in driving limb development, and the ventral portion of the developing limb bud, as previously noted (Ahn et al., 2001; Lyons et al., 1995) (Fig. 1A5, Fig. 2A3 and Fig. 3A3). Notably, expression in the heart AVC peaks at this point. In addition, expression is prominent in subpopulations of cells between the

branchial arches (Fig. 1A5). By E10.5, expression levels have generally declined throughout the head and tail, and are low throughout the gut tube (Fig. 2A4 and Fig. 3A4–5); however, there is still detectable expression in the constricting yolk sac (Fig. 1A6). In addition, expression remains relatively high in the heart AVC (inset, Fig. 2A5), otic vesicle (ov), and branchial arches. Expression is robust in the AER at this stage and appears in an ectodermal patch on the posterior aspect of the forelimbs. Additionally, expression in the ventromedial somites (s) increases, especially in the anterior trunk (Fig. 1A6 and Fig. 2A6).

Bmp4 – E7.5 to E10.5

Bmp4 is expressed in a pattern initially similar to that of *Bmp2*; however, it subsequently varies dynamically throughout early embryogenesis. At E7.25, *Bmp4* like *Bmp2,* is strongly expressed in the yolk sac and allantois, and is concentrated in the anterior part of the embryo, including the cardiac crescent and early neural folds (Fig. 1B1). At E8.25, *Bmp4* remains expressed in the allantois, and strong expression initiates in the posterior lateral plate mesoderm, the AIP, and the sinus venosus (Fig. 1B2). However, yolk sac expression is slightly lower than that of *Bmp2*.

After turning, around E8.75, expression continues to increase in the posterior lateral plate and remains relatively strong in the sinus venosus, the allantois and the caudal most mesoderm of the tail (t) (Fig. 1B3). Again similar to *Bmp2, Bmp4* is detected in the dorsal most tips of the rostral neural tube, albeit at significantly lower levels (Fig. 2B1 and Fig. 3B1), and expression appears in the seam of the diencephalon (d) (Fig. 1B3). Thus, *Bmp2* and *Bmp4* are co-expressed in the AIP, the lateral plate and the neural folds of the head during these earliest stages of embryogenesis (E7.25–E8.75). *Bmp4* has been reported to be more strongly expressed in the myocardium at this time, however using our whole mount method, we detect only low *Bmp4* expression in the heart (Jones et al., 1991). *Bmp4* is expressed strongly in the posterior lateral plate mesoderm, allantois, and yolk sac.

At E9.0, additional domains of *Bmp4* expression appear in many different regions of the embryo (Fig. 1B4 and Fig. 2B2). These domains include the midline seam of the telencephalon, the pituitary infundibulum (pi), the otic vesicle, the rostral somites, the tip and cleft of the branchial arches (b), the thyroid primordium (th), the heart sinoatrial region, the emerging limb buds, the liver, the dorsal optic cup (oc), and the posterior lateral plate mesoderm (Fig. 1B4, Fig. 2B2–3 and Fig. 3B2–3). Additionally, *Bmp4* is expressed in the distal portion of the first branchial arch. Most of these domains are maintained in the E9.5 embryo with marked increase in the rostral dorsal somites, seam of the telencephalon, branchial arches, and in populations of cells likely to be neural crest derived neurons near the branchial arches (Fig. 1B5) (and as shown by (Grotewold et al., 2001). Expression increases in the dorsal portion of the optic cup.

At E10.5, expression of *Bmp4* increases in all these domains, particularly in the telencephalon, the first branchial arch, and around the nasal placode (n), as assessed by intensity of staining by in situ hybridization (Fig. 1B6). Additionally, expression of *Bmp4* is strong in the dorsal somites spanning the length of the embryo, the dorsal gut tube mesoderm, the dorsal aspect of the limb, the outflow tract of the heart (ot), the lung buds (lu) and the limb bud AER (Fig. 1B6, Fig. 2B4–6 and Fig. 3B4–5).

Bmp7 – E7.5 to E10.5

Similar to *Bmp2* and *4*, *Bmp7* expression varies dynamically throughout early embryogenesis. *Bmp7* expression can be observed in many of the same developing tissues as *Bmp2* and *4*, although its levels appear relatively lower during early development. *Bmp7* expression is evident at E7.5 broadly expressed in the cardiac crescent, the allantois, anterior embryonic endoderm, yolk sac, and the anterior primitive streak (Fig. 1C1), as previously described

(Solloway and Robertson, 1999). By E8.25, however, expression remains strong in the yolk sac, but is significantly lower in the AIP, sinus venosus and allantois than either *Bmp2* or *4* (Fig. 1C2). Expression is evident in the dorsalmost portion of the rostral neural folds including strong staining in the ectoderm of the future otic vesicle. In contrast to previous reports, we observe only low levels in the developing heart and allantois (Solloway and Robertson, 1999). By the end of turning, at E8.75, *Bmp7* is prominently expressed in the otic vesicle, telencephalon, the dorsal tip of the neural folds, the future pituitary within the head and a portion of the first branchial arch, while it is present at lower levels in the notochord, heart, somites and the lateral plate mesoderm of the trunk (Fig. 1C3,Fig. 2C1 and Fig. 3C1). Overall, these observations are in agreement with previous reports, except that we detect lower expression in foregut endoderm (Solloway and Robertson, 1999).

By E9.0, *Bmp7* expression continues in these same tissues, however intensifies in the roof of the midbrain, the otic vesicle, telencephalon and branchial arches, with marked expression along the entire length of the developing kidney (mesonephros), while it remains low in the heart (Fig. 1C4, Fig. 2C2 and Fig. 3C2). Expression in the limb buds also initiates at this stage (Fig. 2C3 and Fig. 3C3). By E9.5, expression levels continue to increase in the telencephalon, the dorsalmost neural tube and the heart (Fig. 1C5). New domains of expression also appear, such as the dorsal somites and the gut endoderm (Fig. 1C5 and data not shown). *Bmp7* continues to intensify in the dorsal forebrain, neuroectoderm, lateral plate mesoderm, mesonephros, forelimb bud ectoderm and the neural tube, as previously shown (Solloway and Robertson, 1999). By E10.5, *Bmp7* is relatively strongly expressed in portions of the branchial arches, mesonephros, telencephalon, both fore- and hindlimbs, otic vesicles, dorsal optic cup, and throughout the dorsal somites (Fig. 1C6 and Fig. 2C6). In addition, it is expressed in the gut tube, around both lung buds and posterior stomach (st), as well as in the myocardium of the heart (Fig. 2C4–5 and Fig. 3C2,4–5).

Noggin – E7.0 to E10.5

To assess regions where BMP activity may be regulated by BMP antagonists, we examined the expression of the high affinity BMP inhibitor *noggin*. Similar to Bmp ligand expression patterns, *noggin* transcription occurs in highly restricted embryonic domains. Interestingly, it displays only limited overlap with that of early *Bmp2*, *4* and *7* expression.

At E7.0 *noggin* levels are undetectable in most embryonic tissues, except for strong expression in the node and emerging notochord (Fig. 1D1). Tissues like the allantois, AIP and yolk sac, which co-express Bmp ligands, show no expression of their antagonist *noggin*. At E8.25, *noggin* continues to be expressed in node derivatives and is observed throughout the developing notochord (Fig. 1D2). In fact, we find that at these stages, *noggin* is a robust marker of the early notochordal plate and early notochord. In addition, *noggin* becomes expressed in the dorsal tips of the neural folds, in a pattern that overlaps that of *Bmp2* and *4* (compare Fig. 1A2, B2, D2). At E8.75, following turning, *noggin* expression expands to encompass the entire dorsalmost neural tube, from the tip of the tail to the rostral telencephalon (Fig. 1D3, Fig. 2D1 and Fig. 3D1). In addition, expression begins in the dorsalmost edge of the somites (as previously shown in (Reshef et al., 1998). *Noggin* expression at this stage strongly marks the fusing and fused neural folds, along the entire length of the embryonic axis, and it continues to be maintained in the notochord, although it soon declines in the anterior portion of the embryo.

As development proceeds, at E9.0, *noggin* expression appears at low levels in the dorsal optic cup, the dorsal rostral portion of the somites and more generally throughout the dorsalmost region of the fore- and midbrain, while lower levels are detectable in the liver, as well as the myocardium of the heart (Fig. 1D4, Fig. 2D2–3 and Fig. 3D2). This is in contrast to the high level of *noggin* expression previously reported in the early developing heart (Yuasa et al.,

2005). We observe only low levels of *noggin* in the heart, starting around E8.75. Strikingly, while expression intensifies in the seam of the head and neural tube, it is always absent from the isthmus, the region between the mid- and hindbrain (arrowheads in Fig. 1D3–6 and Fig. 2D1). At E9.5, *noggin* continues to be expressed in the posterior notochord (no), the telencephalon, and the dorsal neural tube, however overall levels in the notochord and neural tube begin to decrease (Fig. 1D5). Expression within the dorsal tip of the somites, however, peaks at this stage. At E10.5, overall *noggin* expression declines slightly from that seen at E9.5. It is expressed in the mesoderm of the lung buds, but is absent from most of the gut tube and heart (Fig. 2D4–5 and Fig. 3D4–5). It also declines in the somites, but remains in the dorsal neural tube (nt) (Fig. 2D6).

Expression of Bmp ligands and *noggin* in developing organs and tissues

Notable overlaps in expression of Bmp ligands and their antagonist *noggin* are observed in developing organs and tissues during organogenesis. The first embryonic regions with overlap of multiple Bmp ligands in post-gastrulation tissues are the allantois, yolk sac and cardiac crescent (compare Fig. 1A1, B1, C1). Shortly thereafter, a similar direct overlap of *Bmp2*, *4*, *7* and *noggin* are all observed in the fusing seam of the telencephalon (with *Bmp2* being weakest and *noggin* being strongest) and in the dorsal most tips of the neural folds, both before and after their fusion into the neural tube (compare Fig. 1A2–4, B2–4, C2–4 and Fig. 2A1–D1).

Bmp co-expression is also evident in the early developing heart. Expression in the heart is initially distinct: *Bmp2* is strongly expressed in the AVC (Fig. 2A2,5 inset and Fig. 3A2); *Bmp4* is localized to both the inflow, or sinus venosus, and the outflow tracts (Fig. 1B3–4, Fig. 2B2,5 and Fig. 3B2); *Bmp7*, in contrast, is found throughout the heart at low levels (Fig. 2C2,5 and Fig. 3C2). However, later during embryogenesis, *Bmp2* continues to be highly localized and robustly expressed within the AVC, while *Bmp4* transcripts increase in the outflow tract and *Bmp7* become more ubiquitous throughout the myocardium (compare Fig. 1A5–6, B5–6, C5–6, Fig. 2 panels 5 and Fig. 3 panels 2). Interestingly, *noggin* is notably absent from the heart at most of these early stages, with only slight and transient expression observed around E9.0 (Fig. 2D2 and Fig. 3D2).

Another tissue showing evident overlap of the Bmp ligands is the limb bud. *Bmp2*, *4*, and *7* are all expressed in the limb bud as previously described (Fig. 2A3, B3, C3 and Fig. 3A3, B3, C3) (Ahn et al., 2001; Francis et al., 1994). *Bmp2* initiates around E9.0 in the ventral ectoderm of the limb bud, as previously noted (Lyons et al., 1995), and can be found shortly thereafter strongly expressed along the AER (Fig. 2A3 and Fig. 3A3). *Bmp4* and *7* are initiated slightly earlier, as the limb bud emerges, and they are more broadly and more strongly expressed throughout both the epithelium and the underlying mesenchyme of the limb bud (Fig. 2B3, C3 and Fig. 3B3, C3). Notably, *noggin* is absent from this domain of Bmp ligand co-expression (Fig. 2D3 and Fig. 3D3).

In somites, all three ligands and their antagonists show dynamic patterns of expression. While they are all expressed at low levels during early somite development, by E9.0, *noggin* and *Bmp4* are expressed robustly in the dorsal portions of the somites, while *Bmp2* and *7* are just initiating low levels of expression (Fig. 1 panels 4 and 5; Fig. 2 panels 3). By E9.5, *Bmp7* and *noggin* become evident in the ventral- and dorsalmost portions of the somites (Fig. 1C6, D6 and Fig. 2C3, D3). Then at E10.5, all three ligands and their antagonist are strongly expressed in nested and overlapping patterns, as follows (Fig. 2 panels 6): *Bmp2*, mid-somite region, stronger in anterior trunk of embryo; *Bmp4*, low ventral somite expression in anterior trunk, robust dorsal somite expression along entire embryonic axis; *Bmp7*, high expression in both the dorsal and ventral domains of the somites, along entire embryonic axis; *noggin*, low expression in ventral portion of somites, stronger expression in dorsal edge of somites, especially in anterior trunk (Fig. 1 panels 6, and Fig. 2 panels 6).

Bmp ligand expression is also striking in the budding organs of the developing gastrointestinal tract. While *Bmp2* is almost undetectable in the foregut (Fig. 2A4 and Fig. 3A4–5), *Bmp4* is expressed in a strikingly unique pattern around the developing midgut (Fig. 2B4 and Fig. 3B4–5). Strong asymmetric expression is observed on the right dorsal side of the gut tube, along the entire length of the dorsal mesogastrium, along the stomach and pancreas (Fig. 2B4 and Fig. 3B4), which winds around the lateral right edge of the developing anterior gut tube. This asymmetric expression is particularly interesting, because it is associated with the coincident breaking of embryonic symmetry (Hecksher-Sorensen et al., 2004), when the pancreas (located posterior to stomach) begins to swing left and the gut tube initiates 'turning'. Expression of *Bmp4* in this region is interesting in that BMPs are known to modulate other extrinsic signals, such as Fgfs, which have been reported in this region (Hecksher-Sorensen et al., 2004) and have been linked to pancreatic development (Bhushan et al., 2001). *Bmp2* is notably absent in this midgut region, while *Bmp7* is strong but symmetrical in the posterior stomach and pancreatic domain (Fig. 2A4, C4 and Fig. 3A4, C4).

During this time, while *Bmp2* is completely absent from the developing lungs, *Bmp4* is strongly expressed in the lung bud mesenchyme and *Bmp7* initiates in the tips of the lung epithelium (Fig. 2A4, C4 and Fig. 3A5, C5). *Noggin*, although expressed at low levels in the distal lung bud mesenchyme, is absent from the epithelium of the lung buds and from the midgut tube (Fig. 2D4 and Fig. 3D4,5). Thus, *Bmp4*, *Bmp7*, and *noggin* are all three expressed in a restricted manner in the lung buds, as previously shown for *Bmp4* (Bellusci et al., 1996), with *Bmp4* and *noggin* primarily in the mesoderm (m), and *Bmp7* in the epithelium (e) (Fig. 3B5, C5, D5).

Relative levels of Bmp and *noggin* expression in different tissues at different stages are compared in Table 1. Overall, we can summarize Bmp ligand expression during early organogenesis as dynamic and often highly localized to distinct tissues and organs during development. As expected, we observe that Bmp ligand expression is particularly enriched in areas where bone growth is required, such as the proximal region of the limb buds, where in addition *noggin* is completely absent. However, we note that *noggin* overlaps in a few domains where multiple individual Bmp ligands are expressed, including the neural tube and somites during early embryogenesis, but is absent from other tissues high in Bmp ligand expression, such as the limb buds, otic vesicle, or most other mesodermal and endodermal derived tissues.

BmpR1a – E7.5 to E10.5

In contrast to the localized and distinct expression patterns of *Bmp2*, *4*, and *7* during early mouse embryogenesis, the BMP receptor *Bmpr1a* is expressed more ubiquitously throughout most embryonic tissues. Expression can be detected at E7.25, albeit at low levels (Fig. 4A1). Around E8.25, slightly increased levels of transcripts can be detected in the neural folds, as well as the lateral plate mesoderm (Fig. 4A2). However, moderate levels of transcripts can be observed throughout the embryo, when compared to controls (Fig. 4A2 and data not shown). By the end of embryonic turning (E8.75), *BmpR1a* is detected in all tissues examined, with the notable exception of the heart atria and ventricle, which have either low or undetectable levels (arrowhead in Fig. 4A3). Increased expression can be seen in the telencephalon, the dorsal neural tube, the pharyngeal endoderm and the first two branchial arches (Fig. 5A1–2 and Fig. 6A1).

At E9.0, expression is still widespread, but has increased from moderate to high levels, with more intense expression detected in the telencephalon, the first branchial arch and the emerging limb bud (Fig. 4A4, Fig. 5A2 and as previously shown in (Dewulf et al., 1995). In addition, higher levels of expression are detected throughout the neural tube, lateral plate mesoderm and limb buds (Fig. 4A4, Fig. 5A3 and Fig. 6A3). Expression continues to appear either low, or absent in the heart myocardium during early heart development (Fig. 4A4, Fig. 5A2 and Fig. 6A2). The increase in limb bud, pharyngeal and neural tube expression intensifies in the

following days, from E9.5 to E10.5 (Fig. 4A5–6). In particular, the anteriormost portion of the head expresses high levels of *BmpR1a* at E10.5. The posterior portion of the tail and most somites also increase expression (Fig. 5A6). As the hindlimbs (hl) appear, expression of *BmpR1a* appears relatively high in this emerging tissue (Fig. 4A6). At these later stages, *BmpR1a* is ubiquitously expressed at lower levels in the stomach, mesogastrium of the stomach, and lung buds (Fig. 4A6, Fig. 5A4 and Fig. 6A4–5).

BmpR1b – E7.5 to E10.5

In contrast to the relatively ubiquitous expression of *BmpR1a*, *BmpR1b* expression is more restricted to specific tissues throughout most of early development. At E7.5 expression is present at low levels throughout the early embryo, but is particularly evident in the forming AIP and the distal yolk sac (Fig. 4B1). This is in contrast to previous findings that *Bmpr1b* expression does not appear until E9.5 (Dewulf et al., 1995). By E8.5, expression is either low or undetectable in most tissues, however localized expression becomes detectable in the developing neural folds (Fig. 4B2), including two distinct patches in the hindbrain, in the region of rhombomere 3 (r3) (Fig. 4B2 inset and Fig. 5B1). Yolk sac, neural tube, rostral neural folds, somites and lateral plate mesoderm are notably devoid of detectable expression. At E8.75, expression continues in the hindbrain and developing otic vesicle and begins to increase in the telencephalon and in the lateral plate mesoderm (Fig. 4B3, Fig. 5B1 and Fig. 6B1).

By E9.0, *BmpR1b* becomes strongly expressed in the anteriormost telencephalon, the optic cup, the first branchial arch and the hindbrain, while expression has appeared at low levels in the dorsal neural tube, the endoderm, the limb buds, the liver and throughout the somites (Fig. 4B4, Fig. 5B2–3 and Fig. 6B2–3). At E9.5, expression increases in the somites, but declines in most of the gastrointestinal tract (Fig. 4B5 and Fig. 5B4). Expression is also observed in the dorsal neural tube, head (hd) and branchial arches as previously shown (Dewulf et al., 1995). This same pattern is mostly maintained through E10.5, when expression is still evident in the head, branchial arches, somites, dorsal neural tube, and with low levels of expression maintained in the limb buds (Fig. 4B6 and previously shown by (Dewulf et al., 1995). Expression in the lungs, gut tube and heart is either low or undetectable (Fig. 4B3–6, Fig. 5B4–5 and Fig. 6B4–5). However, expression continues in both dorsal neural tube and somites (Fig. 5B6).

BmpRII – E7.25 to E10.5

BmpRII expression resembles *BmpR1a* expression in its widespread embryonic distribution. From E7.25 to E8.25, expression is almost negligible, notably lower than either *BmpR1a* or *BmpR1b* (Fig. 4C1–2). However, ubiquitous expression begins after turning, at E8.75 (Fig. 4C3 and previously shown in Bernard et al., 1997). At this stage, *BmpRII* can be found at moderate levels in most tissues, with increased expression in the dorsal rostral neural tube, head, tail, and dorsal region of the somites (Fig. 4C3, Fig. 5C1 and Fig. 6C1). However, like *BmpR1a* and *BmpR1b*, relatively lower levels are observed in the early heart than those observed for Bmp ligands.

At E9.0, expression continues to increase in all tissues, with a marked increase in the anteriormost telencephalon, branchial arches, limb bud and tail tip mesoderm (Fig. 4C4, Fig. 5C2–3 and Fig. 6C2–3). Continued low to negligible levels are observed in the heart (Fig. 5C2 and Fig. 6C2). This expression distribution remains constant through E9.5, with levels increasing in the posterior tail, first branchial arch, developing liver and sinus venosus region (Fig. 4C5). At E10.5, expression is now evident at low levels in the heart myocardium and gut tube (Fig. 4C6, Fig. 5C4–5 and Fig. 6C4–5). Expression in limb buds, both forelimbs and hindlimbs becomes strong by this stage (Fig. 4C6 and Fig. 5C6). In addition, expression in

somites intensifies, albeit diffusely, throughout both the dorsal and ventral portions, along the entire embryonic axis (Fig. 5C6).

Expression of Bmp receptors in developing organs and tissues

Overall, expression of the Bmp receptors is relatively widespread in organs and tissues during early embryonic mouse development. *BmpR1a* and *BmpRII* are expressed ubiquitously in most tissues throughout development, whereas expression of *BmpR1b* displays more restriction to specific tissues. At E8.75, however, all three Bmp receptors are expressed in the fusing neural folds, with each receptor having its own distinct pattern (Fig. 5A1, B1, C1, and Fig. 6A1, B1, C1). For example, *BmpR1a* is enriched in the cephalic region of the neural folds (absent or low in midbrain region), while *BmpR1b* is only observed in a set of small patches within rhombomere 3 of the hindbrain region, and *BmpRII* is expressed throughout the neural folds with increased expression in the dorsalmost neural tube along its length. Similarly, later between E9.5 and E10.5, all three receptors are found in the telencephalon and branchial arches (Fig. 4 panels 5–6 and Fig. 5 panels 2). However, *BmpR1b* and *BmpRII* are strongly expressed in neuroectoderm of the roof of the mouth anlagen, while *BmpR1a* is distinctly absent from this region (Fig. 5 panels 2 and data not shown).

Differences in receptor expression can also be observed in the E10.5 gut tube (Fig. 5 panels 4**,** and Fig. 6 panels 4–5). *BmpR1a* is expressed ubiquitously in all budding organs examined, including the developing lungs and stomach, while *BmpR1b* is completely absent from the lung buds and only slightly expressed in the stomach. Like *BmpR1a*, *BmpRII* expression is widespread in this region, with higher levels near the tips of the lung bud mesoderm and the mesogastrium of the developing gut tube. Interestingly, all three receptors are expressed at notably low to absent levels in the developing heart (Fig. 4A3–6, B3–6, C3–6, Fig. 5 panels 2 and 5, and Fig. 6 panels 2).

Patterns of Bmp receptor gene expression are also distinct, but overlapping in the developing somites. *BmpR1a* is most strongly expressed throughout the somites, from E9.0 to E10.5 (Fig. 5A3, A6). While expression of *BmpR1b* is lower and localized to the medial region of the somites (Fig. 5B3, B6), that of *BmpRII* is more widespread in the somites at E9.0, but becomes slightly enriched in the dorsal portion of the anterior trunk somites by E10.5 (Fig. 5C3, C6).

Nonetheless, Bmp receptors *1a* and *II* display overlaps in expression in many tissues and organs. Both receptors have markedly strong expression in the branchial arches at E9.0 (Fig. 4A4, C4 and Fig. 5A2, C2) and are weakly expressed in the heart throughout development from E8.75 to E10.5 (Fig. 4A3–6, C3–6 and Fig. 5A2, A5, C2, C5). Interestingly, in the limb buds, while *BmpR1a* and *BmpRII* are strongly expressed in the limb mesenchyme, they are notably absent from the ectoderm of the forelimb, including the AER (Fig. 5A3, C3 and Fig. 6A3, C3). This is surprising given reports that describe inactivation of *BmpR1a* in the AER or ventral limb ectoderm, which show that *BmpR1a* is required in this tissue (Ahn et al., 2001; Pajni-Underwood et al., 2007). However, *BmpR1a* possibly plays a greater role in the hindlimbs as these are more severely affected in Msx2-cre;BmpR1a$^{flox/null}$ mutants (Pajni-Underwood et al., 2007). Overall, we could generalize that Bmp receptors are expressed in a more widespread manner than their ligands and display more overlap. When we analyze the expression patterns of both ligand and receptors, we find that ligand expression is not confined to regions that completely overlap with domains of receptor expression, suggesting the possibility that other receptors, such as activin receptors, function to transmit BMP signaling in those regions. Relative levels of Bmp receptor co-expression are summarized in Table 2.

Summary

In this report, we have detailed the expression pattern of several Bmp ligands and their receptor in multiple tissues during murine organogenesis. The Bmp receptor genes, *BmpRII* and *BmpR1a* display largely ubiquitous expression in almost all tissues during embryogenesis; while in contrast, *BmpR1b* expression is more restricted to specific developing tissues such as patches within the hindbrain, otic placode, telencephalon, dorsal neural tube, the first and second branchial arches, limb buds and somites. Bmp ligands, on the other hand, exhibit often highly restricted expression domains that dynamically change patterns in embryonic tissues during their development and are often co-expressed. Generally, *Bmp2* can be summarized to be expressed most strongly in head, heart AVC, limbs, dorsal aorta, and lateral plate mesoderm. *Bmp4* is found in limb buds, lateral plate mesoderm, somites and telencephalon, with a striking asymmetrical expression in the gut mesenchyme. Lastly, *Bmp7* displays robust expression in the limbs, otic vesicle, telencephalon and somites.

Comparison of the spatial expression patterns of ligands and their receptors demonstrates that ligands are often found in tissues where their accepted receptors are either absent or expressed at low levels, such as the heart. This suggests that perhaps ligands in these tissues bind more than one type of receptor, possibly activin receptors. In addition, the limited overlap between Bmp ligands, and *noggin* expression suggests that the few regions of overlap are likely to represent regions of active extracellular regulation by BMP signaling. The number of receptors and ligands that are co-expressed throughout development suggest that several different BMPs, or combinations thereof, are required for the development of various organs during early embryogenesis. This study should help elucidate single Bmp deletion strategies involving Bmp receptors given the observed redundancy of both ligands and other receptors present in regions of expression.

2. Experimental procedures

2.1 Mouse embryos

CD1 embryos were collected from pregnant females (E7.5 through E10.5) after dissection in ice-cold 1xPBS buffer, and then fixed in 4% paraformaldehyde in PBS solution overnight at 4°C with gentle rocking. For embryos E8.75 and older, the amnion was removed during dissection for better probe penetration. Embryos were washed three times in 1xPBS for 10 min at RT and dehydrated using a series of ethanol washes. Embryos were then stored in 70% ethanol at −20°C.

2.2 Whole mount in situ hybridization

For generation of antisense Dig-labeled RNA probes used for in situ hybridization experiments, the following clones were processed as described: pExpress-1-*Bmp2* plasmid was linearized with EcoRV, and anti-sense DIG-RNA probe was made using T7 polymerase. pCMV5Sport6-*Bmp4* was linearized by EcoRI, and anti-sense DIG-RNA probe was made by using T7 polymerase. pCMV5Sport6-*Bmp7* was linearized with SalI and anti-sense DIG-RNA probe was made by using T7 polymerase. pCMV5Sport6-*BmpR1a* was linearized with SalI and anti-sense DIG-RNA probe was made by using T7 polymerase. pCRIITopo-*BmpR1b* was linearized with NotI, and anti-sense DIG-RNA probe was made by using Sp6. pCRIITopo-*BmprII* and pBSSK^{+}-*Noggin* were linearized with HindIII and the anti-sense DIG-RNA probe was made by using T7 polymerase. The reagents were mixed in the following order at room temperature: linearized plasmid (1μg), DIG-RNA labeling mix (Roche 11277073910) 2.0μl, 10x transcription buffer (Roche 1465384) 2μl, Placental ribonuclease inhibitor (Promega N2111) 2μl, RNA polymerase (Roche) 1μl, and double distilled RNase free water to a final volume of 20μl. The mixture was incubated at 37°C for 2 hours. 2μl RQ1 DNase1 was added (Promega

M6101), and then incubated again at 37°C for 15 min. The probes were then purified with Micro Bio-spin colums (Bio-RAD 732-6250). Source of clones used to generate probes were as follows: Open biosystems: *Bmp2* CK792068, *Bmp4* BF538517, *Bmp7* BC010771, *BmpR1a* BC042611, *BmpR1b* BC065106, *BmpRII* from Doug Melton lab (Clone #227), *Noggin* from Jill McMahon with permission from Richard Harland.

Prehybridization solution (50% Formamide (Fisher BP227-100), 5xSSC, pH 4.5, 50μg/ml Ribonucleic acid from torula yeast, TypeVI (Sigma R6625), 1% SDS, 50μg/ml Heparin (Sigma H4784)) was added to probes to a concentration of 10μg/ml, as a stock solution and kept at −80°C. The stock probe was diluted to 1 μg/ml working solution and kept at −20°C. Whole mount in situ hybridization was carried out based on D. Wilkinson's Method (Wilkinson, 1999). Briefly, embryos were treated with 10μg/ml proteinase K (Roche #03115852001) for different time points (E7.5, 5 minutes; E8.5, 10 minutes; E9.0, 15 minutes; E9.5, 20 minutes; E10.5, 30 minutes), re-fixed in a gluteraldehyde/4% paraformaldehyde (PFA) solution, and later prehybridized at 60°C for 1 hour. The samples were transferred into the Digoxigenin-labeled probes and let hybridized overnight. The washing steps were carried out using a Biolane HTI automated incubation liquid handler (Holle & Huttner) as previously described (Villasenor et al., 2008). Images were aquired on an Olympus DP70 camera mounted to a Zeiss NeoLumar microscope.

2.3 Histology

For paraplast sectioning of embryos following in situ hybridization, the embryos were fixed and dehydrated as described above. Embryos were rinsed twice in 100% ethanol for 30 minutes, twice in xylene at room temperature for 10 minutes, 1:1 paraplast:xylene at 60°C for 10 minutes, then a series of 100% paraplast at 60°C (McCormick Scientific 502004), including one overnight. The embryos were then embedded and sectioned with a Reichart Jung microtome. For examination, the sections were mounted on slides (Fisher SuperFrost Plus), deparaffinized in xylene twice for 1 minute each and mounted with coverslips using Permount (Fisher SP15500). Images were acquired on an Axiovert 200M Zeiss inverted fluorescence microscope using an Olympus DP70 camera.

2.4 Expression analysis

Relative expression levels were assessed by visual inspection of the intensity of the chromogenic reaction in the whole mount in situ hybridization and sections of embryos and tissues. Timing of chromogenic reactions were standardized, to allow accurate comparisons of relative transcript levels. Whole mount and section observations were used to describe expression of Bmp ligands and receptors in both the text of this report and the tables presented. Strength of expression intensity was arbitrarily assigned visually by four independent observers. Average expression scores in Tables were calculated from independently assigned values. Embryonic structures identified in text were assessed using structures previously described in a widely referenced embryonic atlas (Kaufman, 1992).

Acknowledgments

We thank Doug Melton and Richard Harland (via Jill McMahon) for providing the *BmprII* and *noggin* clones, respectively. This work was supported by grants JDRF Award 99-2007-472, NIH R01 grant DK079862-01, and the Basil O'Connor March of Dimes Award to OC.

References

Ahn K, Mishina Y, Hanks MC, Behringer RR, Crenshaw EB 3rd. BMPR-IA signaling is required for the formation of the apical ectodermal ridge and dorsal-ventral patterning of the limb. Development 2001;128:4449–61. [PubMed: 11714671]

Bellusci S, Henderson R, Winnier G, Oikawa T, Hogan BL. Evidence from normal expression and targeted misexpression that bone morphogenetic protein (Bmp-4) plays a role in mouse embryonic lung morphogenesis. Development 1996;122:1693–702. [PubMed: 8674409]

Beppu H, Lei H, Bloch KD, Li E. Generation of a floxed allele of the mouse BMP type II receptor gene. Genesis 2005;41:133–7. [PubMed: 15736264]

Beppu H, Minowa O, Miyazono K, Kawabata M. cDNA cloning and genomic organization of the mouse BMP type II receptor. Biochem Biophys Res Commun 1997;235:499–504. [PubMed: 9207184]

Bhushan A, Itoh N, Kato S, Thiery JP, Czernichow P, Bellusci S, Scharfmann R. Fgf10 is essential for maintaining the proliferative capacity of epithelial progenitor cells during early pancreatic organogenesis. Development 2001;128:5109–17. [PubMed: 11748146]

Bitgood MJ, McMahon AP. Hedgehog and Bmp genes are coexpressed at many diverse sites of cell-cell interaction in the mouse embryo. Dev Biol 1995;172:126–38. [PubMed: 7589793]

Christoffels VM, Hoogaars WM, Tessari A, Clout DE, Moorman AF, Campione M. T-box transcription factor Tbx2 represses differentiation and formation of the cardiac chambers. Dev Dyn 2004;229:763–70. [PubMed: 15042700]

Dewulf N, Verschueren K, Lonnoy O, Moren A, Grimsby S, Vande Spiegle K, Miyazono K, Huylebroeck D, Ten Dijke P. Distinct spatial and temporal expression patterns of two type I receptors for bone morphogenetic proteins during mouse embryogenesis. Endocrinology 1995;136:2652–63. [PubMed: 7750489]

Eblaghie MC, Reedy M, Oliver T, Mishina Y, Hogan BL. Evidence that autocrine signaling through Bmpr1a regulates the proliferation, survival and morphogenetic behavior of distal lung epithelial cells. Dev Biol 2006;291:67–82. [PubMed: 16414041]

Eimon PM, Harland RM. In Xenopus embryos, BMP heterodimers are not required for mesoderm induction, but BMP activity is necessary for dorsal/ventral patterning. Dev Biol 1999;216:29–40. [PubMed: 10588861]

Francis PH, Richardson MK, Brickell PM, Tickle C. Bone morphogenetic proteins and a signalling pathway that controls patterning in the developing chick limb. Development 1994;120:209–18. [PubMed: 8119128]

Furuta Y, Piston DW, Hogan BL. Bone morphogenetic proteins (BMPs) as regulators of dorsal forebrain development. Development 1997;124:2203–12. [PubMed: 9187146]

Grotewold L, Plum M, Dildrop R, Peters T, Ruther U. Bambi is coexpressed with Bmp-4 during mouse embryogenesis. Mech Dev 2001;100:327–30. [PubMed: 11165491]

Hecksher-Sorensen J, Watson RP, Lettice LA, Serup P, Eley L, De Angelis C, Ahlgren U, Hill RE. The splanchnic mesodermal plate directs spleen and pancreatic laterality, and is regulated by Bapx1/Nkx3.2. Development 2004;131:4665–75. [PubMed: 15329346]

Hogan BL. Bone morphogenetic proteins in development. Curr Opin Genet Dev 1996;6:432–8. [PubMed: 8791534]

Jones CM, Lyons KM, Hogan BL. Involvement of Bone Morphogenetic Protein-4 (BMP-4) and Vgr-1 in morphogenesis and neurogenesis in the mouse. Development 1991;111:531–42. [PubMed: 1893873]

Kaneko K, Li X, Zhang X, Lamberti JJ, Jamieson SW, Thistlethwaite PA. Endothelial expression of bone morphogenetic protein receptor type 1a is required for atrioventricular valve formation. Ann Thorac Surg 2008;85:2090–8. [PubMed: 18498827]

Kingsley DM. The TGF-beta superfamily: new members, new receptors, and new genetic tests of function in different organisms. Genes Dev 1994;8:133–46. [PubMed: 8299934]

Kretzschmar M, Massague J. SMADs: mediators and regulators of TGF-beta signaling. Curr Opin Genet Dev 1998;8:103–11. [PubMed: 9529613]

Kulessa H, Hogan BL. Generation of a loxP flanked bmp4loxP-lacZ allele marked by conditional lacZ expression. Genesis 2002;32:66–8. [PubMed: 11857779]

Lyons KM, Hogan BL, Robertson EJ. Colocalization of BMP 7 and BMP 2 RNAs suggests that these factors cooperatively mediate tissue interactions during murine development. Mech Dev 1995;50:71–83. [PubMed: 7605753]

Mishina Y, Hanks MC, Miura S, Tallquist MD, Behringer RR. Generation of Bmpr/Alk3 conditional knockout mice. Genesis 2002;32:69–72. [PubMed: 11857780]

Ovchinnikov DA, Selever J, Wang Y, Chen YT, Mishina Y, Martin JF, Behringer RR. BMP receptor type IA in limb bud mesenchyme regulates distal outgrowth and patterning. Dev Biol 2006;295:103–15. [PubMed: 16630606]

Pajni-Underwood S, Wilson CP, Elder C, Mishina Y, Lewandoski M. BMP signals control limb bud interdigital programmed cell death by regulating FGF signaling. Development 2007;134:2359–68. [PubMed: 17537800]

Park C, Lavine K, Mishina Y, Deng CX, Ornitz DM, Choi K. Bone morphogenetic protein receptor 1A signaling is dispensable for hematopoietic development but essential for vessel and atrioventricular endocardial cushion formation. Development 2006;133:3473–84. [PubMed: 16887829]

Reshef R, Maroto M, Lassar AB. Regulation of dorsal somitic cell fates: BMPs and Noggin control the timing and pattern of myogenic regulator expression. Genes Dev 1998;12:290–303. [PubMed: 9450925]

Solloway MJ, Robertson EJ. Early embryonic lethality in Bmp5;Bmp7 double mutant mice suggests functional redundancy within the 60A subgroup. Development 1999;126:1753–68. [PubMed: 10079236]

ten Dijke P, Yamashita H, Sampath TK, Reddi AH, Estevez M, Riddle DL, Ichijo H, Heldin CH, Miyazono K. Identification of type I receptors for osteogenic protein-1 and bone morphogenetic protein-4. J Biol Chem 1994;269:16985–8. [PubMed: 8006002]

Urist MR. Bone: formation by autoinduction. Science 1965;150:893–9. [PubMed: 5319761]

Villasenor A, Chong DC, Cleaver O. Biphasic Ngn3 expression in the developing pancreas. Dev Dyn 2008;237:3270–9. [PubMed: 18924236]

Yamashita H, ten Dijke P, Huylebroeck D, Sampath TK, Andries M, Smith JC, Heldin CH, Miyazono K. Osteogenic protein-1 binds to activin type II receptors and induces certain activin-like effects. J Cell Biol 1995;130:217–26. [PubMed: 7790373]

Yu PB, Beppu H, Kawai N, Li E, Bloch KD. Bone morphogenetic protein (BMP) type II receptor deletion reveals BMP ligand-specific gain of signaling in pulmonary artery smooth muscle cells. J Biol Chem 2005;280:24443–50. [PubMed: 15883158]

Yuasa S, Itabashi Y, Koshimizu U, Tanaka T, Sugimura K, Kinoshita M, Hattori F, Fukami S, Shimazaki T, Ogawa S, Okano H, Fukuda K. Transient inhibition of BMP signaling by Noggin induces cardiomyocyte differentiation of mouse embryonic stem cells. Nat Biotechnol 2005;23:607–11. [PubMed: 15867910]

Zhao GQ. Consequences of knocking out BMP signaling in the mouse. Genesis 2003;35:43–56. [PubMed: 12481298]

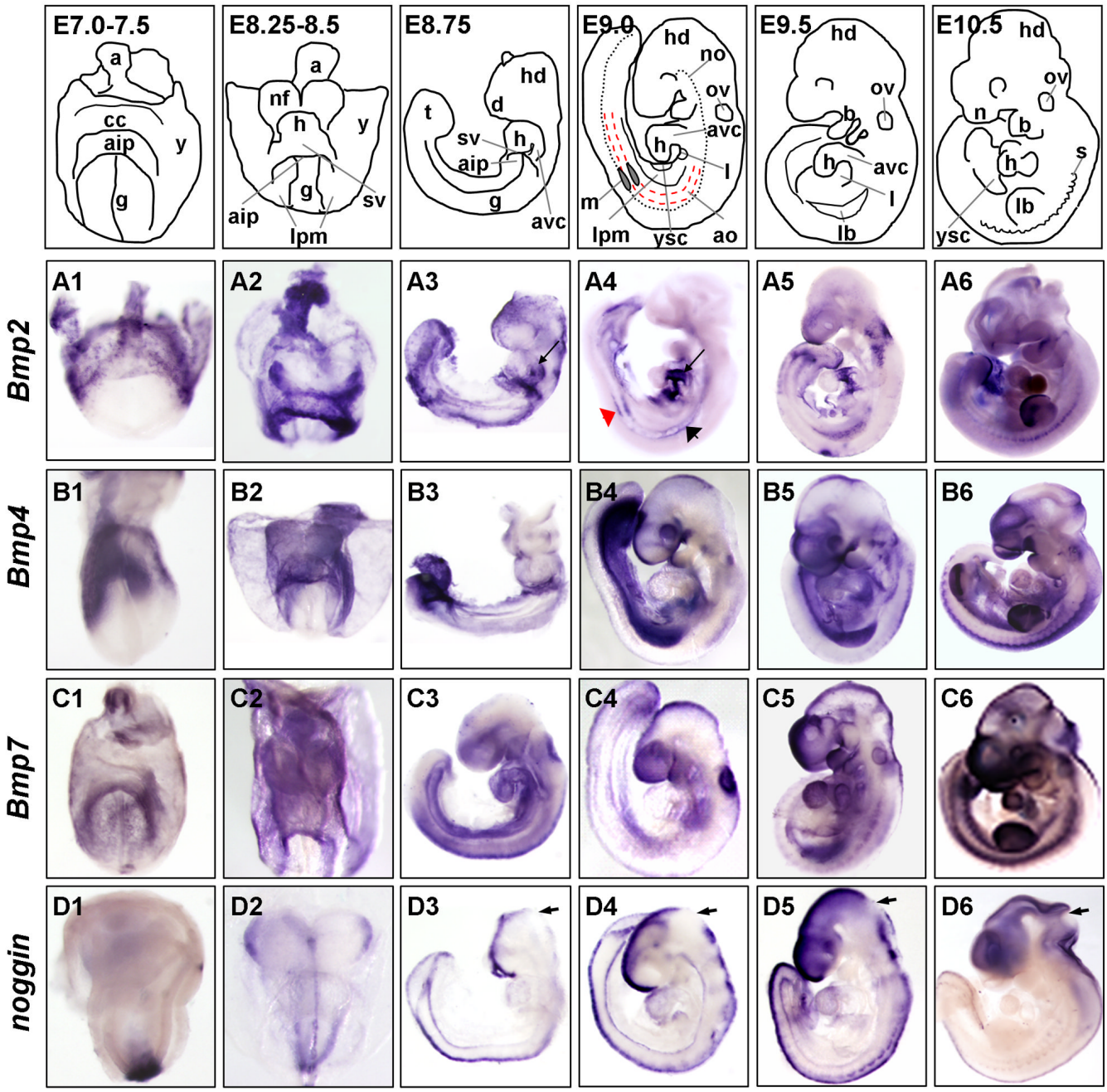

Fig. 1. Expression of Bmp ligands and the BMP antagonist *noggin* during embryogenesis

Whole mount in situ hybridization of embryos E7.5–E10.5 for the following transcripts: Panels A) *Bmp2*; Panels B) *Bmp4*; Panels C) *Bmp7;* and Panels D) *noggin*. Panels 1) E7.0–7.5 embryos are frontal views with head facing forward, allantois in back, pointing up, and yolk sac still attached, except panel B1 which is slightly tilted to the left. Panel A1 and B1 are E7.25, C1 is E7.5 and panel D1 is E7.0. Panels 2) E8.25–E8.5 unturned embryos are shown in frontal views, with head and open AIP facing forward; yolk sac is still attached. Panels 3) E8.75 are shown in process of turning, or shortly after turning. Panels 4–6) E9.0–E10.5 embryos have completed turning and are shown in lateral view facing left. Red dashed lines outline dorsal aorta. All embryos are shown anterior up, dorsal on right. Arrow in panels A3 and A4 indicates

atrioventricular canal (avc); in panel A4, red arrowhead shows mesonephros and black arrowhead points to aorta; small black arrowheads in panels D3–D6 indicate isthmus. Embryonic structures and tissues are annotated in top panel schematics, which represent embryos shown in photographs below. Annotations as follows: a, allantois; aip, anterior intestinal portal; ao, aorta; avc, atrioventricular canal; b, branchial arches; cc, pre-cardiac crescent; d, diencephalon; g, pre-gut endoderm; h, heart; hd, head; l, liver diverticulum; lb, limb bud; lpm, lateral plate mesoderm; m, mesonephros; n, nasal placode; no, notochord; nf, neural folds; ov, otic vesicle; s, somites; sv, sinus venosus; t, tail; y, yolk sac; ysc, yolk sac constriction.

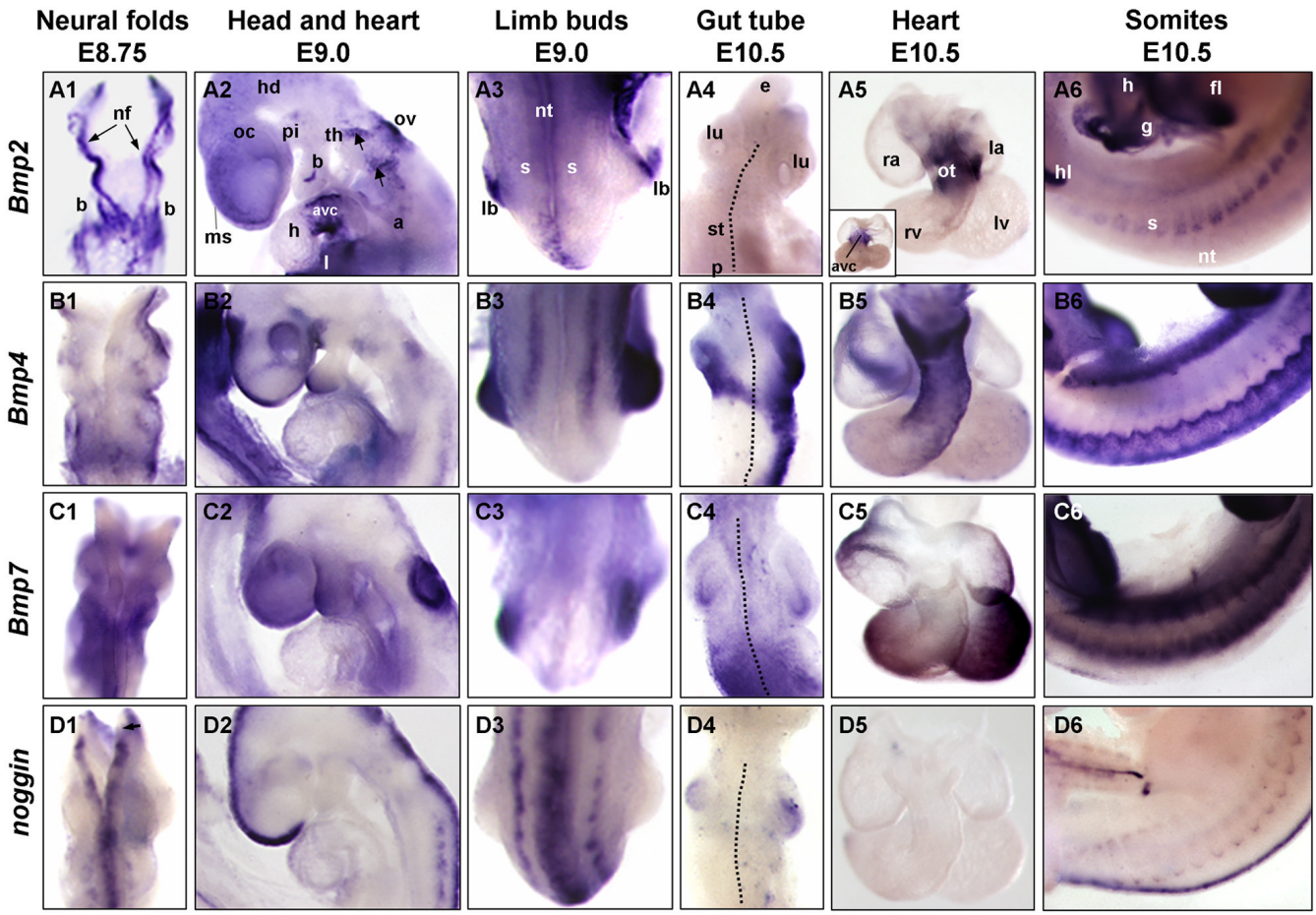

Fig. 2. Expression of Bmp ligands and the BMP antagonist *noggin* in developing tissues

Whole mount in situ hybridization of embryos for the following transcripts: Panels A) *Bmp2*; Panels B) *Bmp4*; Panels C) *Bmp7;* and Panels D) *noggin*. Panels 1) Close up view of embryonic head, showing open neural tube and fusing headfolds at E8.75. Anterior is up, dorsal view. Arrows in A1 point to neural folds. Panels 2) Close up view of anterior portion of E9.0 embryo, highlighting head, heart, sinus venosus, branchial arches, otic vesicle, liver diverticulum and anterior somite expression. Anterior is up, dorsal is on right. Arrows indicate neuron populations. Panels 3) Close up on dorsal midsection of embryo, showing neural tube, anterior somites and developing limb buds at E9.0. View of dorsal surface of neural tube, head is up, tail points away from viewer. Panels 4) Close up view of E10.5 developing gut tube dissected away from the embryo, highlighting expression in esophagus/trachea, lungs, stomach and anterior edge of pancreas. Dotted line indicates dorsal midline of the gut tube. At this stage, the gut tube is beginning to break symmetry and turn left. Anterior is up, dorsal view. Panels 5) Close up views of dissected E10.5 hearts. Ventroanterior view, with outflow tract in front and AVC behind, except inset in A5 where view is dorsoposterior showing *Bmp2* expression in AVC. Note that strong expression in AVC can be seen through transparent outflow tract in main panel A5. Panels 6) Close up view of E10.5 somites (numbers 12–25). Ventral is up, anterior to right, lateral view. Small black arrowhead in panel D1 indicates isthmus. Annotations as follows: a, aorta; avc, atrioventricular canal; b, branchial arches; e, esophagus; fl, forelimb; g, gut; hd, head; h, heart; hl, hindlimb; l, liver diverticulum; la, left atrium; lb, limb bud; lu, lung; lv, left ventricle; ms, midline seam of neural tube; nf, neural folds; nt, neural

tube; oc, optic cup; ot, outflow tract; ov, otic vesicle; p, pancreas; pi, pituitary; ra, right atrium; rv, right ventricle; s, somite; st, stomach; th, thyroid primordium.

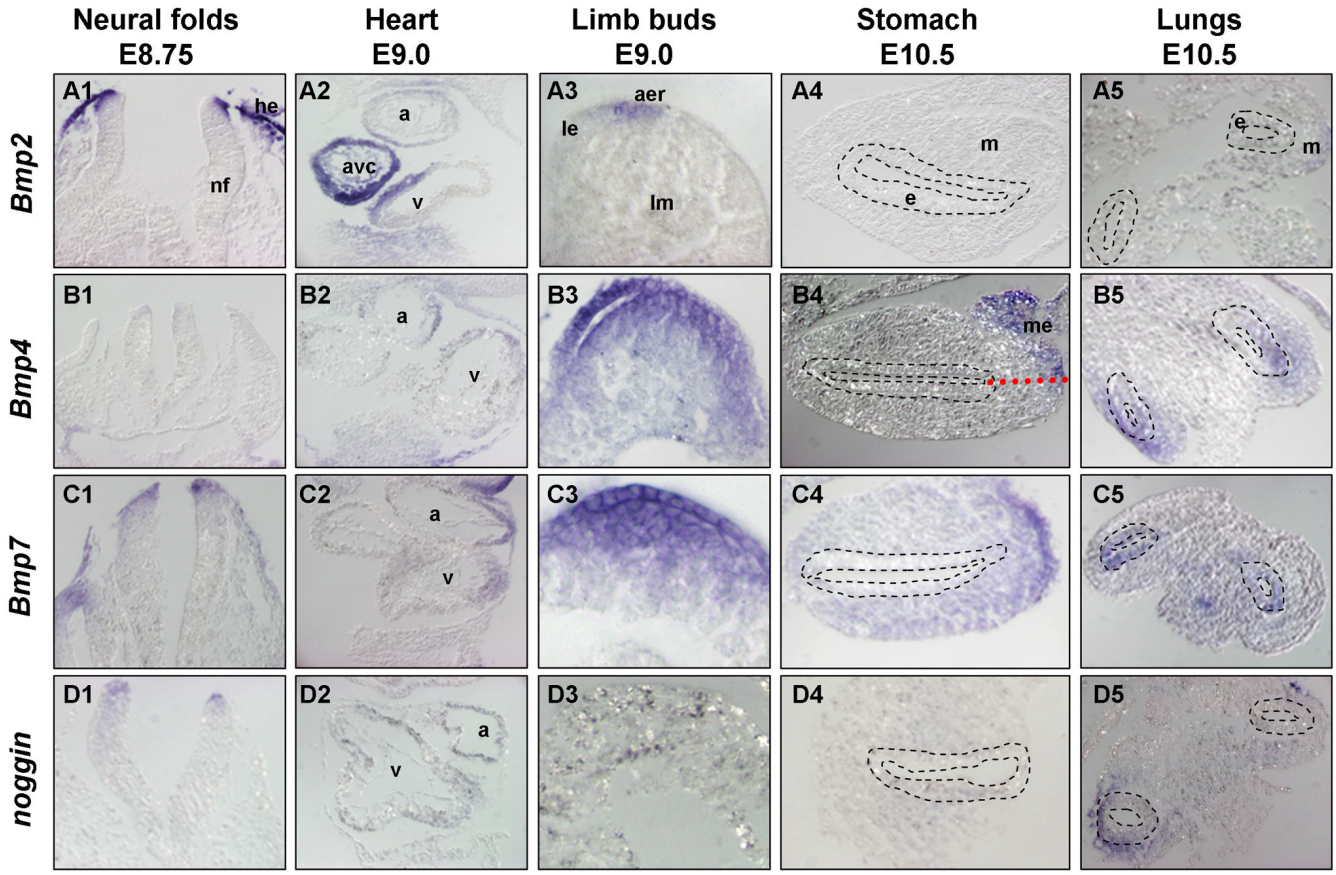

Fig. 3. Sections showing Bmp ligand and *noggin* expression

Sections of whole mount in situ hybridization of embryonic tissues for the following transcripts: Panels A) *Bmp2*; Panels B) *Bmp4*; Panels C) *Bmp7;* and Panels D) *noggin*. Panels 1) Transverse sections of neural tubes and headfolds at E8.75. Dorsal is up. Panels 2) Transverse sections of heart at E9.0 showing both atria and ventricle. Panels 3) Transverse sections through developing limb buds at E9.0, showing outer epidermis (top) and underlying limb mesenchyme. Panels 4) Transverse sections of stomach at E10.5, showing both gut epithelium and gut mesoderm. Stomach epithelium outlined with dashed lines; dorsal is to the right. Red dotted line in panel B4 shows embryonic midline. Panels 5) Transverse sections through developing lung buds. Lung bud epithelium outlined with dashed lines. Anterior is up, dorsal view. Annotations as follows: a, atria; aer, apical ectodermal ridge; avc, atrioventricular canal; e, epithelium; he, head epidermis; le, limb epidermis; lm, limb mesenchyme; m, mesenchyme; me, mesogastrium; nf, neural folds; v, ventricle.

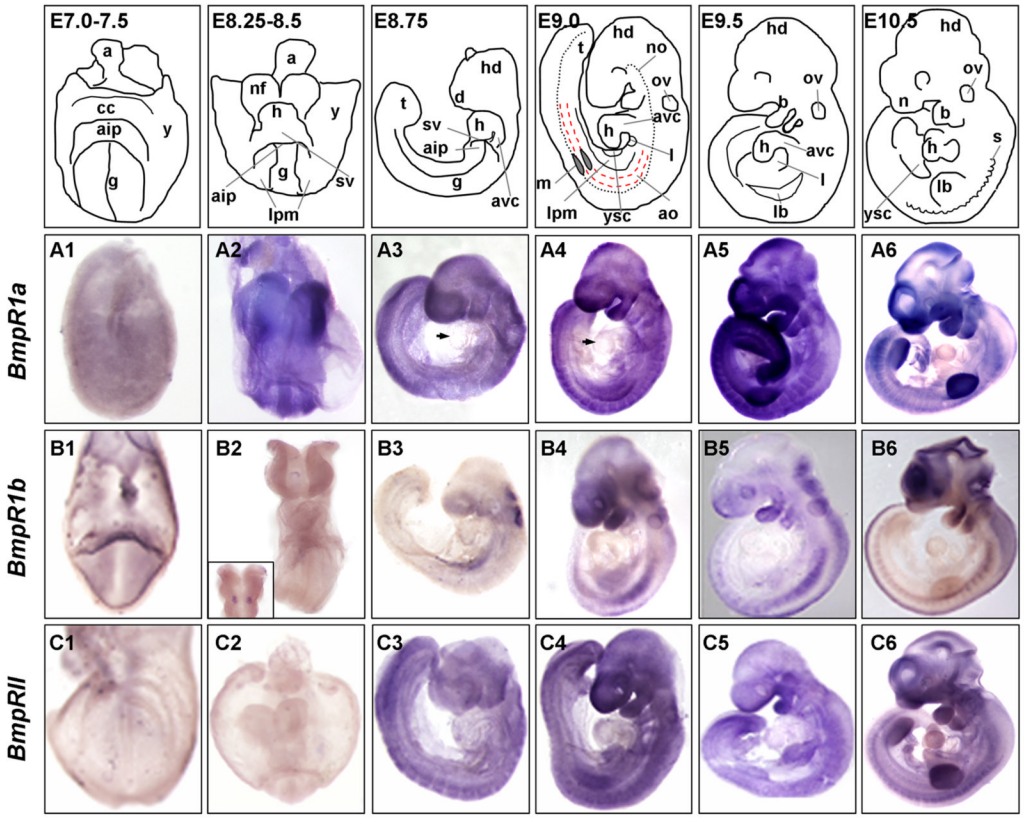

Fig. 4. Expression of Bmp receptors during embryogenesis

Whole mount in situ hybridization of embryos E7.5–E10.5 for the following transcripts: Panels A) *Bmpr1a*; Panels B) *Bmpr1b*; and Panels C) *BmprII*. Panels 1) E7.25–7.0 embryos are frontal views with head facing forward, allantois in back, pointing up, and yolk sac still attached. A1 and C1 are E7.25; B1 is E7.5. Panels 2) E8.25–E8.5 unturned embryos are shown in frontal views, with head and open AIP facing forward: and yolk sac is still attached, except for panel B2 where yolk sac has been removed. In panel B2, inset shows dorsal view and expression in hindbrain rhombomere 3. Panels 3) E8.75 are shown in process of turning, or shortly after turning. Panels 4–6) E9.0–E10.5 embryos have completed turning and are shown in lateral view facing left. All embryos are shown anterior up, dorsal on right. Embryonic structures and tissues are annotated in top panel schematics, which represent embryos shown in photographs below. Arrowheads in A3 and A4 show low levels of expression in heart. Annotations as follows: a, allantois; aip, anterior intestinal portal; ao, aorta; avc, atrioventricular canal; cc, pre-cardiac crescent; d, diencephalon; g, pre-gut endoderm; h, heart; hd, head; l, liver diverticulum; lb, limb bud; lpm, lateral plate mesoderm; m, mesonephros; n, nasal placode; nf, neural folds; ov, otic vesicle; s, somites; sv, sinus venosus; t, tail; y, yolk sac; ysc, yolk sac constriction.

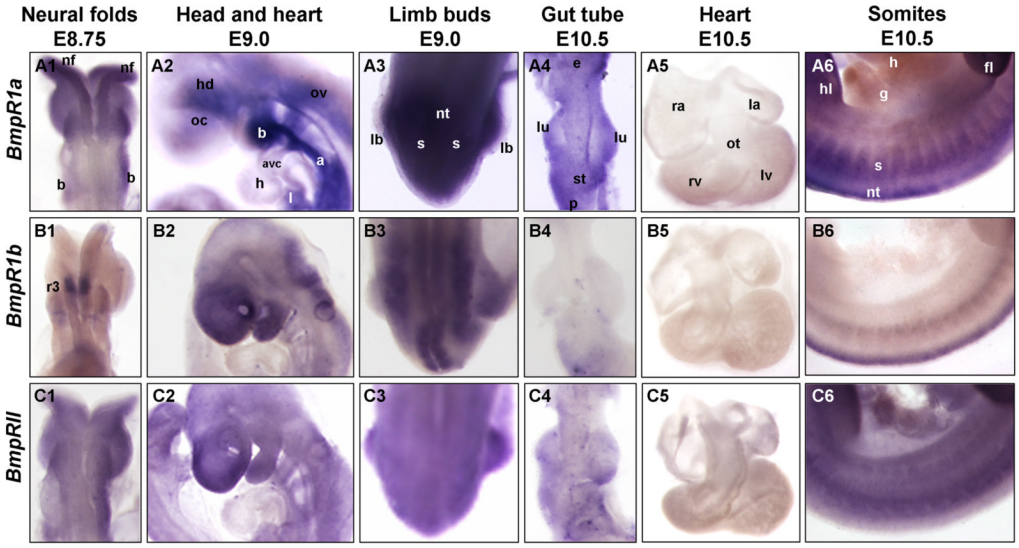

Fig. 5. Expression of Bmp receptors in developing tissues

Whole mount in situ hybridization of embryos for the following transcripts: Panels A) *Bmpr1a*; Panels B) *Bmpr1b*; and Panels C) *BmprII*. Panels 1) Close up view of embryonic head, showing open neural tube and fusing headfolds at E8.75. Anterior is up, dorsal view. In panel B1, r3 indicates rhombomere 3. Panels 2) Close up view of anterior portion of E9.0 embryo, highlighting head, heart, sinus venosus, branchial arches, otic vesicle, liver and anterior somite expression. Anterior is up, dorsal is on right. Panels 3) Close up on dorsal midsection of embryo, showing neural tube, anterior somites and developing limb buds at E9.0. View of dorsal surface of neural tube, head is up, tail points away from viewer. Panels 4) Close up view of E10.5 developing gut tube dissected away from the embryo, highlighting expression in esophagus/trachea, lungs, stomach and anterior edge of pancreas. At this stage, the gut tube is beginning to break symmetry and turn left. Anterior is up, dorsal view. Panels 5) Close up views of dissected E10.5 hearts. Ventroanterior view, with outflow tract in front and AVC behind. Panels 6) Close up view of E10.5 somites (numbers 12–25). Ventral is up, anterior to right, lateral view. Annotations as follows: a, aorta; avc, atrioventricular canal; b, branchial arches; e, esophagus; fl, forelimb; g, gut; hd, head; h, heart; hl, hindlimb; l, liver diverticulum; la, left atrium; lb, limb bud; lu, lung; lv, left ventricle; nf, neural folds; nt, neural tube; oc, optic cup; ot, outflow tract; ov, otic vesicle; p, pancreas; ra, right atrium; rv, right ventricle; s, somite; st, stomach.

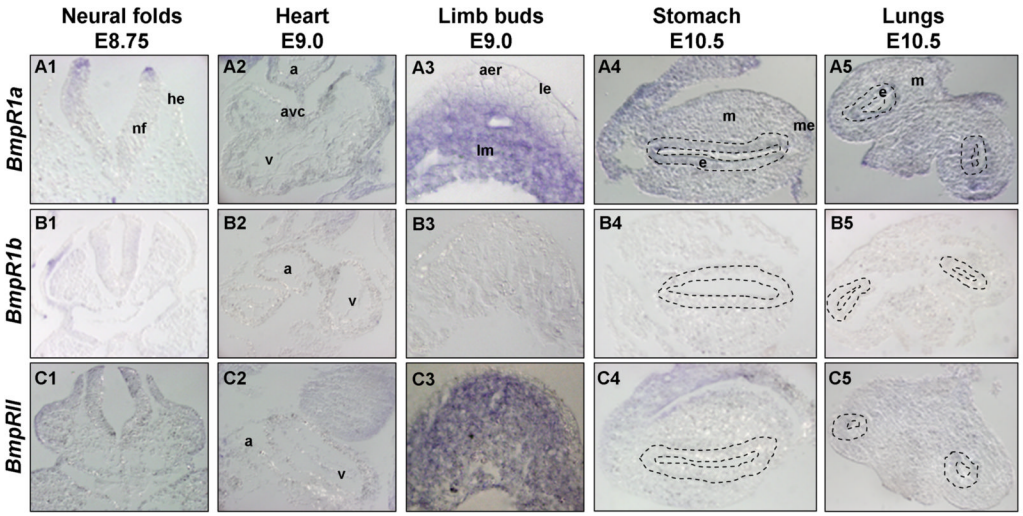

Fig. 6. Sections showing Bmp receptor expression

Sections of whole mount in situ hybridization of embryonic tissues for the following transcripts: Panels A) *Bmpr1a*; Panels B) *Bmpr1b*; and Panels C) *BmprII*. Panels 1) Transverse sections of neural tubes and headfolds at E8.75. Dosal is up. Panels 2) Transverse sections of heart at E9.0 showing both atria and ventricle. Panels 3) Transverse sections through developing limb buds at E9.0, showing outer epidermis and underlying limb mesenchyme. Panels 4) Transverse sections of stomach at E10.5, showing both gut epithelium and gut mesoderm. Stomach epithelium outlined with dashed lines; dorsal is to the right. Panels 5) Transverse sections through developing lung buds. Lung bud epithelium outlined with dashed lines. Anterior is up, dorsal view. Annotations as follows: a, atria; aer, apical ectodermal ridge; avc, atrioventricular canal; e, epithelium; he, head epidermis; le, limb epidermis; lm, limb mesenchyme; m, mesenchyme; me, mesogastrium; nf, neural folds; v, ventricle.

Table 1

Summary of Bmp ligand and *noggin* expression

Relative expression of Bmp ligands and *noggin* during embryogenesis. Relative in situ intensities were determined from whole mount in situs of *Bmp2*, *Bmp4*, *Bmp7* and *noggin* for various tissues during organogenesis (embryonic stages E8.75, E9.0, E10.5). (−) absent, (+) weak, (+++) medium, and (+++++) strong expression. (N/A refers to absence of structure at specific embryonic stage, i.e. not developed yet, or past development).

	Bmp2			***Bmp4***			***Bmp7***			***noggin***		
	E8.75	**E9.0**	**E10.5**	**E8.75**	**E9.0**	**E10.5**	**E8.75**	**E9.0**	**E10.5**	**E8.75**	**E9.0**	**E10.5**
Neural folds	++++	N/A	N/A	+	N/A	N/A	++	N/A	N/A	+++	N/A	N/A
Head												
Telencephalon	+	+	++	+	++	+++	++	+++	++++	−	++	+++
Seam	+	+	+	+	+++	++	+	+++	++++	++++	++++	++++
Midbrain	++	++	+	+	+	+	+	+	++	+	++	+++
Hindbrain	++	+	+	−	−	++	−	+	+++	+	++	+++
Heart	++	++	+++	+	+	+++	+++	++	++++	+	+	−
Lung	N/A	N/A	−	N/A	N/A	++++	N/A	N/A	++	N/A	N/A	+
Stomach	N/A	N/A	−	N/A	N/A	++++	N/A	N/A	+++	N/A	N/A	−
Limb buds	N/A	+++	++++	N/A	+++++	++++	N/A	+++	+++++	N/A	−	−
Somites	+	+	++	++	+	++++	+	+	++++	+	++	+

Table 2

Summary of Bmp receptor expression

Relative expression of Bmp receptors during embryogenesis. Relative in situ intensities were determined from whole mount in situs of *BmpR1a*, *BmpR1b*, and *BmpRII* for various tissues during organogenesis (embryonic stages E8.75, E9.0, E10.5). (−) absent, (+) weak, (+++) medium, and (+++++) strong expression. (N/A refers to absence of structure at specific embryonic stage, i.e. not developed yet, or past development).

	BmpR1a			***BmpR1b***			***BmpRII***		
	E8.75	**E9.0**	**E10.5**	**E8.75**	**E9.0**	**E10.5**	**E8.75**	**E9.0**	**E10.5**
Neural folds	+++	N/A	N/A	++	N/A	N/A	++	N/A	N/A
Head									
Telencephalon	++++	+++	++++	+	+++	++++	++	+++	+++
Seam	+++	+	++	+++	−	+	++	++	++
Midbrain	+++	++	+	−	+	++++	+	++	++
Hindbrain	++	++	++	++	++	++	+	+	+
Heart	+	+	+	+	+	+	+	+	+
Lung	N/A	N/A	+++	N/A	N/A	−	N/A	N/A	++
Stomach	N/A	N/A	+++	N/A	N/A	+	N/A	N/A	++
Limb buds	N/A	++++	++++	N/A	++	+	N/A	+++	++++
Somites	++	+++	+++	−	+++	++	++	++	+++